$M_{4,5}N_{4,5}N_{4,5}$ Auger decay spectra of the resonantly excited $3d^9 4f$ configuration of xenonlike ions in solids

R. Ruus, A. Kikas, A. Maiste, E. Nõmmiste, and A. Saar
Institute of Physics, Estonian Academy of Sciences, Riia 142, EE-2400 Tartu, Estonia

M. Elango
Department of Experimental Physics and Technology, Tartu University, Ülikooli 18, EE-2400 Tartu, Estonia and Institute of Physics, Estonian Academy of Sciences, Riia 142, EE-2400 Tartu, Estonia

J. F. van Acker, M. Qvarford, J. N. Andersen, and R. Nyholm
Department of Synchrotron Radiation Research, Lund University, Sölvegatan 14, S-223 62 Lund, Sweden

I. Martinson
Department of Atomic Spectroscopy, Lund University, Sölvegatan 14, S-223 62 Lund, Sweden
(Received 17 September 1993; revised manuscript received 17 January 1994)

The synchrotron-radiation-induced Auger and photoelectron spectra of the xenonlike ions I^- (in CsI), Cs^+ (in CsI), Ba^{2+} (in BaF_2), and La^{3+} (in LaF_3) have been measured in the vicinity of the $M_{4,5}$ absorption edges of these ions. It is shown that the spectra of La and Ba measured at $3d^{10} \rightarrow 3d^9 4f$ resonances exhibit a very intense $4f$-spectator structure which changes its energy and intensity with the energy of the exciting photons. Calculation of the Auger decay of the $3d^{-1}4f$ configuration shows that this structure is due to transitions to the $4d^{-2}4f + 4p^{-1}$ final ionic configuration, the high-energy part of which overlaps the $4d^{-2}$ continuum. In the case of Ba this structure coexists with the normal Auger structure which appears as a result of the $M_4 M_5 N_{6,7}$ Coster-Kronig transitions. The spectra of I^- contain only the normal $M_{4,5}N_{4,5}N_{4,5}$ Auger structure related to the $3d^{-1} \rightarrow 4d^{-2}$ transitions. The spectra of Cs^+ are similar to those of I^- with a small admixture of the $4f$-spectator-like structure.

I. INTRODUCTION

Recent progress in synchrotron-radiation and electron-spectroscopy techniques has led to the development of a powerful method, the resonant Auger electron spectroscopy (RAES), which exposes the details of the decay dynamics of excited configurations of atoms, molecules, and solids.[1] One of the systems for which this method has given interesting insights is the excited configuration $2p^{-1}3d$ of argonlike ions Cl^-, K^+, Ca^{2+}, and Sc^{3+} in ionic solids.[2] There, the $3d$-spectator-electron-related structure appears in the $L_{23}M_{23}M_{23}$ Auger spectra at the resonant $2p \rightarrow 3d$ excitation with progressing collapse of the $3d$ orbital. With increasing photon energy this structure shifts linearly to higher kinetic energies indicating that the "photon-absorption–Auger-decay" process, usually taken as a two-step process, should be considered here as a single Auger-resonant inelastic-scattering event.[3]

Another case where such phenomena could be expected is the decay of the $3d^{-1}4f$ configuration of xenonlike ions. For $3d$ core-hole states the dominant decay channel is known to be the $M_{45}N_{45}N_{45}$ Auger transition.[4] At the resonant $3d \rightarrow 4f$ photoexcitation, the corresponding spectator Auger structure should be very sensitive to the degree of localization of the $4f$ orbital both in the initial $3d^{-1}4f$ and final configurations. As has been shown by experimental and theoretical studies of the M_{45} x-ray-absorption (XAS) and emission spectra of xenonlike ions in ionic solids,[5,6] the collapse of the $4f$ wave function occurs for the $3d^{-1}4f$ configuration when proceeding from Xe to Cs^+ and Ba^{2+}. The near-edge structure of M_{45} absorption is rather simple and well understood, thereby allowing unambiguous selective generation of $3d^{-1}4f(J=1)$ states with synchrotron radiation. However, the final $4d^{-2}4f$ ionic configuration of the Auger decay is much less investigated for these ions, although it has attracted a fairly large attention in connection with its role in forming the $4p$ x-ray photoemission spectra (XPS) of neighboring atoms to Xe.[7] Theoretical estimations predict the $4f$ orbital collapse for the $4d^{-2}4f$ configuration to start from Xe.[8] It is obvious that direct experimental observation of the $3d^{-1}4f \rightarrow 4d^{-2}4f$ Auger transition in resonant Auger spectra is anticipated. Quite recently, several papers have been published on $4d$ core-hole-related Auger transitions for Xe-like ions in halogenides after resonant $4d \rightarrow 4f$ excitation.[9,10] They offer much information about the $4d^{-1}4f(J=1)$ states.

We measured the energy distribution curves (EDC) of ejected electrons of CsI, BaF_2, and LaF_3 in the region of $M_{45}N_{45}N_{45}$ Auger transitions of iodine, cesium, barium, and lanthanum ions, respectively, by varying the photon excitation energy stepwise through the M_{45} absorption structure of these ions. The spectra show drastic changes of the decay pattern of the $3d^{-1}$ excitations in this sequence of ions. In iodine all observed spectra contain

only the "normal" structure related to $3d^{-1} \rightarrow 4d^{-2}$ Auger transitions. On the contrary, the resonantly excited spectra of La and Ba exhibit a very intensive new structure which changes its energy and intensity with excitation energy, being undoubtedly induced by the $4f$ spectator electron. The spectra of Cs are similar to those of I besides a small admixture of the "spectator" structure. A theoretical calculation of the decay of the $3d^{-1}4f$ states shows that the resonant structure for La^{3+} and Ba^{2+} is due to transitions to the strongly interacting $4d^{-2}4f$ and $4p^{-1}$ final ionic configurations. However, for Ba^{2+} the situation seems to be more complicated: the "normal" and "spectator" structures coexist. The weak "spectator" structure in the case of Cs is apparently caused by Auger shakedown transitions from the intermediate $3d$-core-hole states (with an excited electron on the near-edge continuous εf or/and resonantly localized $4,\varepsilon f$ orbitals) to the states of final ionic $4d^{-2}4f$ configuration. It should be noted that though the measurements were performed with solid ionic samples, the free-ion approximation turned out to be successful to explain the main features and trends of the spectra. The solid-state effects are essential for the borderline situation in cesium and barium spectra.

II. EXPERIMENT

The measurements are carried out using synchrotron radiation from beamline 22 at the MAX-laboratory, Lund University, Sweden.[11] The electron spectra are excited by a photon beam from a modified SX-700 plane-grating monochromator with an energy resolution 0.5–0.8 eV (in the energy range 600–900 eV), and analyzed by a hemispherical electron spectrometer Scienta SES-200 at an energy resolution of 0.3 eV. The M_{45} absorption spectra are obtained in the electron yield mode. Other experimental details have been described earlier.[2]

The thin films ($\sim$200 Å) of CsI, BaF_2, LaF_3 are prepared by thermal evaporation from a molybdenum boat onto a polished stainless-steel substrate in a preparation chamber at a pressure of 10^{-7} Torr, and then transferred to the experimental chamber, operated at 10^{-10} Torr.

The measured EDC's of ejected electrons are normalized to the incident photon flux. The kinetic and binding energies are given relative to the bottom of the conduction band of the sample using the band gap energies 6.2 eV for CsI,[12] 11.0 eV for BaF_2,[13] and 9.4 eV for LaF_3.[14]

III. THEORETICAL CONSIDERATIONS

The analysis of the complicated spectra observed turned out to be practically impossible without thorough theoretical evaluation of the main nonradiative decay processes involved. The final interpretation is based on autoionization spectra calculated using the procedure described earlier.[2] Here we make some general remarks.

We approximate the inner-shell excitation and its Auger decay as a two-step process. The calculations are essentially atomic and are based on the Hartree-Fock (HF) method to obtain the atomic wave functions. Relativistic effects are taken into account as corrections of the order α^2 (α is the fine-structure constant).[15] Calculations in the intermediate coupling scheme with Slater integrals found from HF treatment of the $4d^{-2}$ final state are shown to overestimate the term separations of multiplets.[16] Therefore, for a better agreement with the observed spectra we reduce the radial Coulomb F_k ($k>0$) exchange G_k and R_k integrals for the open $4d^{-2}4f$ and $4d^{-2}$ shells by 20%.

Our preliminary calculations indicate that the region of electron energies connected with "normal" $3d^{-1} \rightarrow 4d^{-2}$ and "spectator" $3d^{-1}4f \rightarrow 4d^{-2}4f$ Auger processes is overlapped by the $M_{45}N_{23}O_{23}$ processes (especially in Ba^{2+} and La^{3+}) and by "participator" $3d^{-1}4f \rightarrow 4p^{-1}$ transitions. Since the single-configuration evaluation predicts the $M_{45}N_{23}O_{23}$ transition rates to be much smaller than the $M_{45}N_{45}N_{45}$ ones (this is confirmed by the experimental Auger spectra of Xe where these structures are sufficiently separated[4]) we neglected the $M_{45}N_{23}O_{23}$ contributions in our final calculations. The same cannot be done with the $3d^{-1}4f \rightarrow 4p^{-1}$ channel since, due to $4f$-orbital collapse, the interaction of $4d^{-2}4f$ and $4p^{-1}$ configurations is expected to be so strong[8] that they cannot be considered separately. So we have treated them together, and the corresponding transitions $3d^{-1}4f \rightarrow 4p^{-1}+4d^{-2}4f$ have been calculated in a configuration-superposition approximation. The direct photoionization transitions $4p^6 \rightarrow 4p^{-1}+4d^{-2}4f$, the energies of which coincide with those of the $M_{45}N_{45}N_{45}$ Auger electrons, have very small cross sections at the resonant $3d \rightarrow 4f$ energies and thus we neglect them.

As the measurements are not performed with free ions but with solid samples there arises a serious problem of how to include the solid-state effects into the calculations. We have done this by using the Watson sphere model which reduces the influence of surrounding ions to a spherically symmetric correction to the atomic potential.[17] The depth of this additional potential well is taken equal to the value of the Madelung potential on the ion site, i.e., ± 6.4 eV for I^- and Cs^+ in CsI, -17.6 eV for Ba^{2+} in BaF_2, and -25.8 eV for La^{3+} in LaF_3.[18]

The influence of the Watson sphere correction on the radial part of the wave functions is rather small. However, in the case of the $3d^{-1}4f$ configuration of Cs^+ the radial part of the $4f$ wave function crucially depends on the value of the Watson correction; if the latter is smaller than -5.2 eV then the mean $4f$ radius abruptly changes from 1.5 to 17 a.u.

Another important effect of these corrections is the decrease of the energy separations between the final configurations $4d^{-2}$ and $4d^{-2}4f+4p^{-1}$. In the case of Ba^{2+} in BaF_2 this effect leads to overlapping of these widely spread configurations, as can be seen from Table I. The extent of this overlap affects the corresponding low-kinetic-energy part of the calculated spectator structure of Ba^{2+} (as demonstrated in Sec. IV D).

In Table I the computed values of the binding energies, E_B^{th}, of actual configurations of cations are presented in comparison with our experimental data, E_B. We compute the binding energies in crystals as $E_0 - E_p$ for singly

TABLE I. Experimental (E_B) and calculated (E_B^{th}) binding energies (in eV). E_B values are referred to the bottom of the conduction band.

Ions		Configurations $3d_{3/2}^{-1}$	$3d_{5/2}^{-1}$	$4p^{-1}$	$4d^{-2}4f+4p^{-1}$	$4d^{-2}$
Cs free ions	E_B^{th}	753.4	739.7	172.0	172.0–202.8	194.6–205.2
Cs in CsI	E_B^{th}	745.1	731.4	163.7	163.7–194.6	178.0–188.6
	E_B	745.2	731.3	163.4		
Ba free ions	E_B^{th}	820.0	805.0	201.0	201.0–234.8	243.4–254.8
Ba in BaF_2	E_B^{th}	800.9	785.8	181.8	181.8–215.6	204.8–216.2
	E_B	802.0	786.7	179.7		
La free ions	E_B^{th}	890.3	873.8	232.1	232.1–268.6	296.6–308.8
La in LaF_3	E_B^{th}	862.5	846.0	204.5	204.5–241.1	241.4–253.6
	E_B	856.8	840.0	201.5		

ionized final states and as E_0-2E_p for doubly ionized final states (e.g., for $4d^{-2}$ configuration). Here E_0 is the difference of the total energies of ground ($^1S_0$) and final states of the ions in the Watson sphere. For polarization energies, E_p, we use the estimated values of 1.9 eV for Cs^+ in CsI (Ref. 19) and 2.0 eV for Ba^{2+} in BaF_2.[20] We calculate the polarization energy for La^{3+} in LaF_3 by using a classical electrostatic approach[21] in which

$$E_p=\frac{e^2}{2d}\left[1-\frac{1}{\varepsilon_\infty}\right]$$

for an ion in a dielectric solid. Here ε_∞ is the dielectric constant and d the effective hole radius ($d=0.9R$ for a hole on a cation site, R being the nearest-neighbor distance). Using the values $R=2.38$ Å (Ref. 22) and $\varepsilon_\infty=2.56$,[23] we obtain $E_p\cong 2$ eV. As seen, the experimental and theoretical values for absolute binding energies (and their differences) of the $3d$ and $4p$ levels of CsI and BaF_2 agree well with each other. Some mismatch (up to 6 eV) between the theoretical and experimental data for LaF_3 is probably due to the larger degree of covalency of this compound.

IV. RESULTS AND DISCUSSION

Observed EDC's of LaF_3, BaF_2, and CsI are given in Figs. 1–4. The insets show the near-edge structures of the M_{45} absorption spectra of these compounds. The upper curves of each figure (labeled as N) show the "normal" $M_{45}N_{45}N_{45}$ Auger spectra excited by photons with energies far above the M_{45} thresholds, in the region of comparatively small absorption coefficients. Therefore, the normal Auger spectra have considerably smaller intensities than the EDC's excited at near-edge regions. For simultaneous display in the figures the intensities of the normal spectra are strongly increased in comparison with the resonantly excited EDC's which are normalized to equal photon flux. The normal spectra are compared with calculated $3d^{-1}\rightarrow 4d^{-2}$ transition intensities. The resonantly excited spectra are labeled by capital letters A, B, C, etc., corresponding to the exact excitation energies as marked in the insets. Before examining the resonantly excited spectra we will briefly discuss the absorption and "normal" Auger spectra.

A. Absorption spectra

The M_{45} absorption spectrum of I in CsI (Fig. 4) is very similar to that of gaseous Xe,[24] except for the absence of weak $3d\rightarrow np$ features. The broad near-edge bands correspond to transitions of $3d$ electrons to the εf continuum and they may be considered as shape resonances. In contrast, the spectra of La and Ba (Figs. 1 and 2) are dominated by two intense sharp $^3D_1(M_5)$ and $^1P_1(M_4)$ lines caused by $3d\rightarrow 4f$ transitions separated by the spin-orbit interaction of the $3d$ subshell. The appearance of these lines and their insensitivity to different chemical surroundings have been considered as major

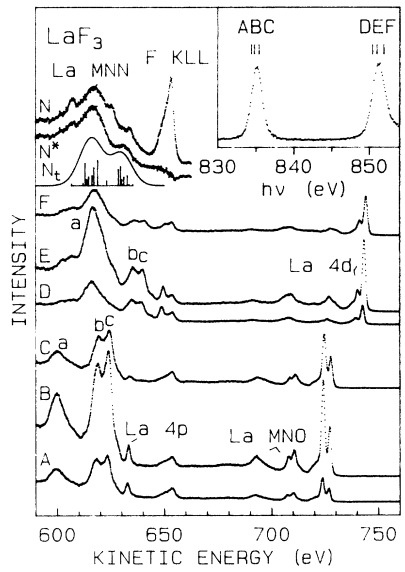

FIG. 1. EDC's for LaF_3. The resonantly excited spectra are normalized to equal photon flux. The La M_{45} absorption edge is shown in the inset. The capital letters at each EDC correspond to the vertical bar with the same letter in the inset and show the photon energy used. The energy levels and corresponding Auger transitions are indicated for most of the structures. The labels a, b, and c indicate features discussed in the text. N is the normal Auger spectrum excited by 900-eV photons. N^* is the normal Auger spectrum after subtraction of the F KLL Auger spectrum. N_t is the calculated La^{3+} $M_{45}N_{45}N_{45}$ Auger spectrum broadened with a Gaussian of 11-eV FWHM.

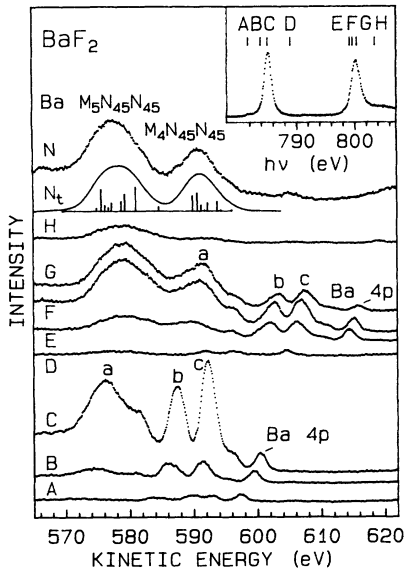

FIG. 2. The same as Fig. 1 for BaF_2. The normal Auger spectrum is excited by 880-eV photons, the calculated spectrum is broadened with a Gaussian of 5-eV FWHM.

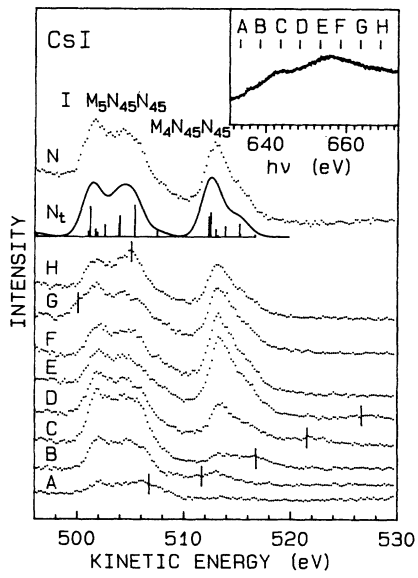

FIG. 4. The same as Fig. 1 for I in CsI. The normal Auger spectrum is excited by 800-eV photons, the calculated spectrum is broadened with a Gaussian of 2-eV FWHM. The positions of the Cs $4p$ photoline in spectra H and G, and of the I $4p$ photoline in spectra $A-E$ are indicated by vertical bars.

evidence of $4f$ localization in these atoms.[5] The M_4 line is broader than the M_5 one, having a clearly asymmetric shape, which is caused by interference between "direct" M_5 photoemission to the continuum and emission via creation and $M_4M_5N_{67}$ Coster-Kronig decay of the M_4 autoionizing state.[25] The shape of the near-edge absorption of Cs (Fig. 3) is intermediate between these two cases displaying features of both of them. The nature of main M_4 and M_5 bands cannot be strictly related neither to $3d \rightarrow \varepsilon f$ ionization nor to localized $3d \rightarrow 4f$ excitation. These excitations are usually referred to as transitions to resonantly localized continuum states, often labeled as $4,\varepsilon f$ states. The appearance of such states is known to be a common feature of $4d \rightarrow 4f$ excitations with a collapsing $4f$ orbital.[26]

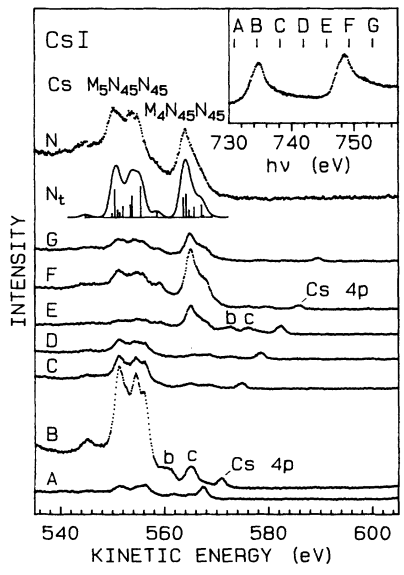

FIG. 3. The same as Fig. 1 for Cs in CsI. The normal Auger spectrum is excited by 850-eV photons, the calculated spectrum is broadened with a Gaussian of 2-eV FWHM.

B. Normal Auger spectra

We start by discussing the $M_{45}N_{45}N_{45}$ "normal" Auger spectra of I^- and Cs^+ in CsI (Figs. 3 and 4) which are very similar to each other. They contain well-separated M_5 and M_4 groups with some fine structure. The computed $3d^{-1} \rightarrow 4d^{-2}$ spectra (assuming statistical 6:4 population of initial M_5 and M_4 core-hole states) with a Gaussian broadening of 2 eV quite satisfactorily reproduce the experimental results. Our photon-excited spectrum for solid CsI closely resembles the spectra of the CsI molecule and the Cs atom, obtained by electron excitation.[27] The difference in linewidth of about 0.5 eV between atomic and solid phases is well understood by the usual solid-state broadening factors. For Ba in BaF_2 (Fig. 2) the M_4 and M_5 groups are well separated, also, but their fine structure has practically vanished. A theoretical reproduction of the spectra can only be achieved using a convolution width as large as about 5 eV, which is somewhat surprising because for Ba metal it has been possible to extract the $3d^{-1} \rightarrow 4d^{-2}$ structure with a fitting linewidth of about 1.5 eV.[28] On the other hand, the analogous spectrum of atomic Ba is shown to be anomalously wide.[29] This large broadening has been attributed to the configuration-interaction effects involving the outer atomic valence $6s^2$, $6s5d$, $5d^2$ electrons. Our measured normal Auger spectrum of Ba in BaF_2 in Fig. 2 resembles the fine-structure envelope of that of atomic Ba.

An even more drastic broadening is observed for La in LaF_3 (Fig. 1). Here the *MNN* spectrum of La is superimposed on the KLL spectrum of F. We present the curve N^* as a purified version of the La spectrum which is obtained by subtracting the normal Auger spectrum excited by photons with energy 790 eV (below the M_{45} threshold of La) from the curve N excited by photons with energy 900 eV (above the M_{45} threshold). The theoretical $3d^{-1} \rightarrow 4d^{-2}$ spectrum can be matched with the experimental one only with a broadening of more than 10 eV. Such a broadening even tends to smear out the separation of the M_4 and M_5 groups.

The computed Auger total widths of $3d^{-1}$ ionic states and photoexcited $3d^{-1}4f\,(J=1)$ states with collapsed $4f$ electrons are given in Table II for the relevant free ions. Our value for Xe is in a good accord with the results of Ref. 30 (0.68 eV), exceeding by about 30% the experimental value [0.5 eV (Ref. 31)]. The widths of $3d^{-1}4f$ states are larger than those of the $3d^{-1}$ ones, mainly due to the contribution of the participator $3d^{-1}4f \rightarrow 4d^{-1}$ channel.

The comparison of the computed widths and experimental XPS and XAS widths for the M_5 line clearly indicates that the observed shape of $M_{45}N_{45}N_{45}$ spectra of Ba and La cannot be understood in terms of conventional broadening factors (lifetime, phonon interaction, etc.). For Ba we can only state that, since the $M_{4,5}$ photoemission lines do not show any anomalous broadening or splitting, we have to relate the MNN broadening to the final-state effects, the origin of which remains to be understood.

For La the situation is somewhat different. As known, the creation of single-core-hole states of La in its compounds may be accompanied by relaxation processes involving the electron transfer from the valence shell of neighboring atoms to the La $4f$ level.[32] This effect is thought to account for the splitting of the $M_{4,5}$ photoline[33] and appearance of the $3d^{-1}4f \rightarrow 5p^{-1}4f$ lines in x-ray emission[34] of LaF_3. It is quite reasonable to assume the possibility of such screening processes also for two-core-hole ionic states. Then the observed $M_{45}N_{45}N_{45}$ spectrum of La probably reflects a superposition of transitions between properly weighted different initial $(3d^{-1}, 3d^{-1}4f)$ and final $(4d^{-2}, 4d^{-2}4f, 4d^{-2}4f^2)$ configurations which may lead to a strong extra broadening.

TABLE II. The computed Auger-decay total width (in eV) for $3d^{-1}$ initial state $\Gamma(3d^{-1})$ and the widths $\Gamma(^3D_1)$ and $\Gamma(^1P_1)$ for the photoexcited $3d^{1-}4f(^3D_1)$ and $3d^{-1}4f(^1P_1)$ initial states, respectively.

Ions	$\Gamma(3d^{-1})$	$\Gamma(^3D_1)$	$\Gamma(^1P_1)$
I^-	0.61		
Xe	0.65		
Cs^+	0.7	0.74	0.77
Ba^{2+}	0.75	0.81	0.89
La^{3+}	0.8	0.86	0.96

In this connection we turn the attention to another anomaly related to the La $M_{45}N_{45}N_{45}$ spectrum. According to our data, the position of the $M_5N_{45}N_{45}$ band on the kinetic-energy scale shifts rather smoothly with increasing atomic number Z, i.e., by about 25 ± 1 eV per unit change of Z. The corresponding energy values are 503 eV for I in CsI, 552 eV for Cs in CsI, and 577 eV for Ba in BaF_2. For the preiodine elements In, Sn, Sb, Te in metallic phase this shift was observed to be 26 ± 0.5 eV,[16] which agrees well with the value given above. However, going from Ba in BaF_2 to La in LaF_3 this shift is about 40 eV. The difference of ~ 15 eV is too large to be ascribed to the usual chemical shift. This anomaly seems to indicate that for an extra hole of La in LaF_3 there exists a strong screening process of solid-state origin, such as the above-mentioned charge-transfer relaxation, which affects both the initial and final Auger-state energies. Its main contribution is likely to come from the final state. This statement is supported by earlier studies of lanthanide metals where the relaxation energies for the two-hole states were found to be much larger than for the simple one-hole states.[35]

This solid-state-relaxation shift is important for the analysis of the RAES spectra as well. For the "spectator" decay of configurations with a collapsed $4f$ electron, the relaxation energies are close to those for single-core-hole states. For systems with large two-hole relaxation energies the free-ion and solid-state situations differ strongly. In a free ion the "normal" and "spectator" features are well separated, but in a solid the "normal"-like structure may be shifted to overlap the "spectator" structure, which therefore cannot be unambiguously identified. It can also be noted that the energy separation between "normal" and "spectator" features may differ between the same type of ion in different type of solids (see also Ref. 36).

C. Resonantly excited spectra: La in LaF_3

We start the examination of resonantly excited $M_{45}N_{45}N_{45}$ spectra with $La^{3+}(LaF_3)$ in which case the $4f$ orbitals are certainly collapsed, both in core-excited initial and final states, and the $3d$ photoabsorption resonances represent the $3d^{-1}4f$ excitations. Figure 1 shows a set of on-resonance EDC's in a wide energy region which also contains La $4d$ and $4p$ XPS photolines and La *MNO* and F *KLL* Auger bands. Using the latter as an intensity reference we can clearly see the strong resonant enhancement of the photolines and the significant changes in the $4d_{3/2}$:$4d_{5/2}$ branching ratio which indicates a high probability and strong term dependence of the $3d^{-1}4f \rightarrow 4d^{-1}$ autoionization. A similar phenomenon is observed for other Xe-like ions studied here, also, and it will be discussed in a separate paper.[37]

In the region of the La *MNN* transitions a strong and well-developed structure appears which vanishes off-resonance and drastically differs from the normal La $M_{45}N_{45}N_{45}$ bands. This resonant $M_{45}N_{45}N_{45}$ structure consists of a broadband "*a*" and a doublet of close-lying bands, "*b*" and "*c*," accompanied by several weaker shoulderlike features, as most distinctly revealed on the

curve B of Fig. 1. These bands are wider than the $4p$ photoline, but significantly narrower than the normal M_5 band of La. The common observation for all resonant EDC's of La is that with increasing photon energies the whole resonant structure shifts linearly to higher kinetic energies, thus resembling the behavior of usual photoelectron lines.

The absence of any similarity between the resonant MNN structure and the normal spectrum makes the latter quite useless for the interpretation of resonant bands. The resonant decay features are spread over more than 30 eV, expanding around the normal counterpart on both high- and low-energy sides. The position of the band "a" on curve B is especially noticeable, this band lies more than 15 eV lower than the normal M_5 band. Obviously, the resonant $3d^{-1}4f$ excitations decay to a very complicated manifold of final states.

In Figs. 5(a) and 5(b) we compare the observed on-resonance spectra with the calculated $3d^{-1}4f(J=1)\rightarrow 4d^{-2}4f+4p^{-1}$ spectra. On the energy scale the experimental and theoretical curves are aligned by the $4p$ photoline. As seen, the computed curves well reproduce the major features of the observed resonant structure, both energetically and in intensity. The theory

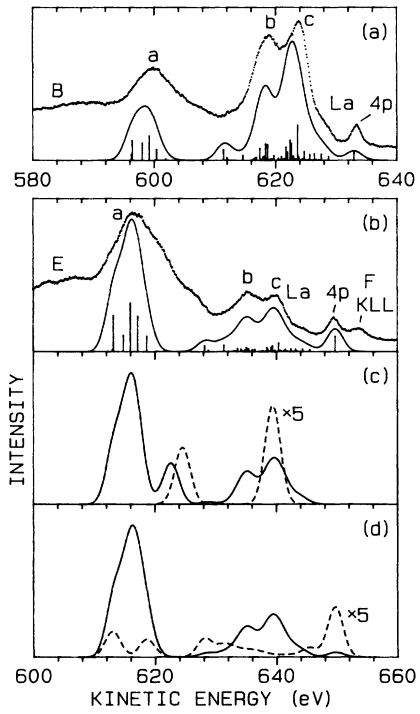

FIG. 5. Resonant $M_{45}N_{45}N_{45}$ Auger spectra for LaF_3 as compared to the calculation of the Auger transitions (a) $3d^{-1}4f(^3D_1)\rightarrow 4d^{-2}4f+4p^{-1}$ and (b) $3d^{-1}4f(^1P_1)\rightarrow 4d^{-2}4f+4p^{-1}$. In (a) and (b) are shown the spectra B and E of Fig. 1, respectively. In (c) and (d) are shown the calculated Auger $3d^{-1}4f(^1P_1)\rightarrow 4d^{-2}4f$ (solid line) and $3d^{-1}4f(^1P_1)\rightarrow 4p^{-1}$ (dashed line) spectra in the single-configuration approximation (c) and in configuration-interaction approximation for Auger final ionic states $4d^{-2}4f+4p^{-1}$ (d). All computed spectra are broadened with a Gaussian of 3-eV FWHM.

confirms the composite nature of the main resonant bands and the dominance of upper $4d^{-2}4f$ final states in the M_4 decay.

The M_4 on-resonance spectrum (curve E) turns out to be a replica of the M_5 one, shifted energetically exactly by the corresponding increase of the photon energy, with a redistribution of intensities in favor of the band "a" well reproduced by the theory. Curve E shows some weak low-energy structure at $\sim 10-15$ eV from band "a." We tentatively ascribe it to the $M_{45}N_{23}O_{23}$ transitions. Our calculations show that the intensity of the band "a" is mainly caused by the transitions $3d^94f(^1P)\rightarrow 4d^84f+4p^5$ and the intensities of the bands "b" and "c" by the transitions $3d^94f(^3D)\rightarrow 4d^84f+4p^5$, if we describe the initial $3d^94f$ configuration in the pure LS coupling scheme. Whereas for the M_5 and M_4 excitations the main components of the intermediate-coupling eigenvectors correspond to the ^3D and ^1P terms, respectively, band "a" is favored at the M_4 excitation and bands "b" and "c" are favored at the M_5 excitation, in accordance with the measured spectra.

The main uncertainty seems to be connected with the large widths of the measured bands, especially of band "a." Solid-state hybridization and screening effects, discussed in Sec. III, may be important here as well. We cannot exclude the possibility that in the real LaF_3 crystal the upper levels of the $4d^{-2}4f$ multiplet lie slightly above the $4d^{-2}$ ionization limit, contrary to the predictions of Table I. Then a new double Auger-decay route $3d^{-1}4f\rightarrow(4d^{-2}4f)\rightarrow 4d^{-2}$ may be opened and affect the shape of the spectrum in the vicinity of band "a." The proper theoretical description of such processes requires much more sophisticated models and calculation procedures than those used in present work.

Thus, the theoretical analysis allows us to attribute the resonant structures of La $M_{45}N_{45}N_{45}$ Auger spectra to the $3d^{-1}4f(J=1)\rightarrow 4d^{-2}4f+4p^{-1}$ transitions. Our calculations show that both in Ba^{2+} and La^{3+} the partial width of the $3d^{-1}4f\rightarrow 4d^{-2}4f$ transitions, the most intensive of the 20 possible decay channels, yields about 43% of the total Auger width of the $3d^{-1}4f$ ($^3D_1$) photoexcited state. The partial width of the $3d^{-1}4f\rightarrow 4p^{-1}$ participator decay is term dependent, having the values of 1.7% for $^3D_1(M_5)$ and 2.3% for $^1P_1(M_4)$ excitations. To demonstrate the relative roles of the spectator and participator channels we present in Figs. 5(c) and 5(d) their contributions to the $^1P_1(M_4)$ excitation in the single-configuration and multiconfiguration ($4d^{-2}4f+4p^{-1}$) approximations. As seen, the single-configuration approach quite satisfactorily describes the main features of the observed resonant structure, but it totally fails to reproduce a participator channel. Thus, strictly speaking, the La resonant structure should be considered as a result of the mixed "spectator-participator" decay of the $3d^{-1}4f$ configuration. However, the relatively small contribution of the participator component justifies the pure spectator approach.

D. Resonantly excited spectra: Ba in BaF_2

The major features of the resonant spectra of $Ba^{2+}(BaF_2)$, presented in Fig. 2, are quite similar to those

of La. The $4p$ photoline is followed by the strong doublet "b"-"c" and the broad low-energy band "a," and even the weaker shoulderlike features seen in La spectra are present here. This three-band resonant structure moves linearly with exciting photon energy as a photoemission feature and is nicely repeated on the M_4 resonance. However, the latter has an additional, broad strong low-energy band which is absent in the La case. This band has the same width as the normal $M_5N_{45}N_{45}$ band, and nearly the same energy which does not change with photon energy. Therefore, it can be attributed to the normal $M_5N_{45}N_{45}$ channel, opened by the $M_4M_5N_{67}$ Coster-Kronig decay. The constant high-kinetic-energy shift (about 2 eV) of this band is most probably related to post-collision-interaction (PCI) of a slow Coster-Kronig and a fast Auger electron.

Thus, the general similarity of the RAES of photoexcited $3d^{-1}4f$ states of $Ba^{2+}(BaF_2)$ and $La^{3+}(LaF_3)$ is evident. However, closer examination reveals some important differences. While the relative intensity and energy separation of the bands "b" and "c" are for Ba nearly the same as for La, their widths ($\sim$2.8 eV) are significantly smaller. However, relative intensity and position of "a" have changed: the "a-b" separation for Ba is 11 eV while it is 19 eV for La. Another peculiarity of band "a" is that by tuning the photon energy its intensity changes in a different way than that of bands "b" and "c." So, the observed MNN resonant structure seems to consist of two parts, the high-energy region of relatively narrow bands "b," "c," and the low-energy region of band "a."

In Fig. 6, the observed on-resonance $M_{4,5}$ spectra are compared with computed $3d^{-1}4f \rightarrow 4d^{-2}4f + 4p^{-1}$ spectra. The calculations reasonably well reproduce the high-energy region of the measured spectra, but, unlike the case of La, there is a clear mismatch in the low-energy region which cannot be compensated for by the reduction of electrostatic integrals. Our calculations

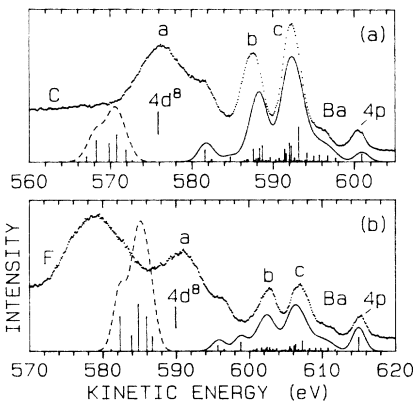

FIG. 6. Resonant $M_{45}N_{45}N_{45}$ Auger spectra for BaF_2 as compared to the calculation of the Auger transitions (a) $3d^{-1}4f(^3D_1) \rightarrow 4d^{-2}4f + 4p^{-1}$ and (b) $3d^{-1}4f(^1P_1) \rightarrow 4d^{-2}4f + 4p^{-1}$. In (a) and (b) are shown the spectra C and F of Fig. 2, respectively. The dashed part of the computed spectra corresponds to the $4d^{-2}4f$ states with energies lying above the $4d^{-2}$ threshold (labeled by the vertical bars). The computed spectra are broadened with a Gaussian of 2-eV FWHM.

show that measured band "a" lies at the energies where the $4d^{-2}$ threshold is expected to be found. In Fig. 6, these thresholds, i.e., the lowest-binding-energy states of $4d^{-2}$ ionic configuration are marked as vertical bars on the kinetic-energy scale by using the data of Table I and the theoretical $3d^{10} \rightarrow 3d^9 4f$ excitation energies (788.7 eV for $^3D_1$ and 803.8 eV for $^1P_1$ states). The $4d^{-2}4f$ states with energies above this threshold (dashed parts of theoretical curves) are thus allowed to delocalize and seem not to contribute to the resonant structure. So, theory gives a suitable explanation to the above-made empirical division: the region of relatively narrow resonant bands corresponds to the $4d^{-2}4f$ states lying below the $4d^{-2}$ limit. Only these bands could be considered as the true $4f$ spectator features. They exhibit only small changes going from La to Ba since the Z dependence of the $3d^{-1}4f \rightarrow 4d^{-2}4f$ transitions with collapsed $4f$ orbital for isoelectronic ions is rather weak.

The interpretation of the broad low-energy band "a" is, however, much more complicated. Our theoretical results allow us to suggest that band "a" is induced by the $3d^{-1}4f \rightarrow 4d^{-2}$ Auger shakeofflike transitions. These transitions are expected to have energies slightly lower than the $3d^{-1} \rightarrow 4d^{-2}$ transitions. As seen in Fig. 2, band "a" nearly coincides with its "normal" counterpart at on-resonance conditions. On the other hand, it has a different shape than the "normal" band which is broader by at least 2.5 eV. However, the proper theoretical solution of this problem is beyond our model.

E. Resonantly excited spectra: Cs and I in CsI

The resonant spectra of Cs^+ (Fig. 3) and I^- (Fig. 4) are completely different from those of La and Ba. They are dominated by "normal" photon-energy-independent $M_4N_{45}N_{45}$ and $M_5N_{45}N_{45}$ structures shifted slightly (by $\sim$1 eV for Cs and $\sim$0.5 eV for I) to higher energies, most probably by PCI effects (in curves G and H the M_5 band of iodine is slightly distorted by the overlapping Cs $4p$ photoline). The situation is fully understandable in the light of the nature of the near-edge $3d$ excitations of I and Cs: as the $4f$ orbital is not collapsed, the $3d^{-1} \rightarrow 4d^{-2}$ transitions dominate in the resonantly excited MNN spectra. In this sense our RAES data once more confirm that the $M_{4,5}$ near-edge absorption bands of these ions are caused by transitions to above-threshold states.

However, the resonant spectra of Cs contain two additional weaker bands which are most pronounced on the curves B and E of Fig. 5. Their relative positions (between the $4p$ photoline and corresponding normal MNN bands) and widths (about 2.1 eV) as well as the photon energy dependence closely follow the behavior of the $4f$ spectator bands "b" and "c" of Ba and La. So it is natural to suggest that they also belong to a $4f$-spectator-like structure. The calculation of $3d^{-1}4f \rightarrow 4d^{-2}4f + 4p^{-1}$ spectra for Cs^+ assuming a collapsed $4f$ orbital (as in the free Cs^+ ion case), fully supports this suggestion. The other possible interpretation of those bands, namely, that they are part of the direct $4p$ photoionization spectra of Cs, can be ruled out since they are clearly stronger than

the main $4p$ line, whereas for atoms with $Z \sim 54-57$ the low-energy features of the $4p$ XPS high-binding-energy satellite structure are much weaker than the main line.[38] So, we have to conclude that the observed resonant *MNN* spectra of Cs^+ contain simultaneously $3d^{-1} \rightarrow 4d^{-2}$ and $3d^{-1}4f \rightarrow 4d^{-2}4f$-like structures, in other words, the $M_{4,5}$ near-edge photoexcitations of Cs^+ exhibit both continuous ($3d \rightarrow \varepsilon f$) and localized ($3d \rightarrow 4f$) character.

This dualistic nature of the $3d$ excitations of Cs has been earlier observed in the $M_{4,5}$ x-ray emission of Cs in CsCl.[6] Now we may add that the RAES, indeed, seems to be a very sensitive technique for discovering and investigating such "partially localized" excitations, especially since it can be experimentally performed in a more straightforward way than the electron-excited resonant x-ray emission (re-emission) measurements. In our case the apparent localization of the excited-state electron may be considered as a result of the interaction of a low-energy εf photoelectron with a fast Auger electron leading to the recapture of the photoelectron by the ionized core and, subsequently, to the shakedownlike transitions $3d^{-1}\varepsilon f \rightarrow 4d^{-2}4f$. A similar explanation was used to interpret the ion yield spectra of Ar near its $L_{2,3}$ thresholds.[39]

V. CONCLUSIONS

We have measured the energy distribution curves of ejected electrons of CsI, BaF_2, and LaF_3 in the region of $M_{45}N_{45}N_{45}$ Auger transitions of xenonlike iodine, cesium, barium, and lanthanum ions, by varying the energy of the exciting photons stepwise through the M_{45} absorption structure of these ions. The spectra show drastic changes of the decay pattern of $3d^{-1}$ excitations in this sequence of isoelectronic ions. For I all spectra observed contain only the normal $M_{45}N_{45}N_{45}$ Auger structure related to the $3d^{-1} \rightarrow 4d^{-2}$ transitions. In contrast, the spectra of La and Ba, excited at their $3d^{10} \rightarrow 3d^9 4f$ resonances, exhibit a very intensive new structure which changes its energy and intensity with the energy of exciting photons and is induced by the spectator $4f$ electron. In the case of Ba this structure coexists with the normal Auger structure the latter appearing as a result of the $M_4M_5N_{67}$ Coster-Kronig transitions. The spectra of Cs are similar to those of I, but a small admixture of the spectator structure is also seen at resonance excitation, however. It is caused by the Auger shakedown transitions from intermediate states with excited electron in the near-edge continuous εf or/and resonantly localized $4,\varepsilon f$ orbitals.

Theoretical calculation of the decay of the $3d^{-1}4f$ configuration shows that the resonant structure for Ba^{2+} and La^{3+} is to be ascribed to transitions to the $4d^{-2}4f + 4p^{-1}$ final configuration. Its shape is influenced by the solid-state modifications of the energy separation between the final configurations $4d^{-2}$ and $4d^{-2}4f + 4p^{-1}$. In a fully consistent picture the resonance excitation and following decay should be described as a single Auger-resonant inelastic-scattering event.

ACKNOWLEDGMENTS

This work was supported by the Swedish Natural Sciences Research Council, the Estonian Science Foundation, the Crafoord Foundation, and the Royal Swedish Academy of Sciences. The authors wish to thank Dr. A. Ausmees for his assistance in analysis of the spectra.

[1]Several papers on this topic have recently appeared in the *Proceedings of the 2nd International Workshop on Auger Spectroscopy and Electron Structure (IWASES-II), Malmö, Sweden, 1991,* edited by K. Wandelt, C.-O. Almbladh, and R. Nyholm [Phys. Scr. **T41** (1992)].

[2]M. Elango, A. Ausmees, A. Kikas, E. Nõmmiste, R. Ruus, A. Saar, J. F. van Acker, J. N. Andersen, R. Nyholm, and I. Martinson, Phys. Rev. B **47**, 11 736 (1993).

[3]T. Åberg, Phys. Scr. **T41**, 71 (1992).

[4]L. O. Werme, T. Bergmark, and K. Siegbahn, Phys. Scr. **6**, 141 (1972).

[5]A. A. Maiste, R. E. Ruus, S. A. Kuchas, R. I. Karaziya, and M. A. Elango, Zh. Eksp. Teor. Fiz. **78**, 941 (1979) [Sov. Phys. JETP **51**, 474 (1980)].

[6]P. Motais, E. Belin, and C. Bonnelle, Phys. Rev. B **25**, 5492 (1982).

[7]G. Wendin, *Structure and Bonding* (Springer, Berlin, 1981), Vol. **45**, p. 1, and references therein.

[8]H. Smid and J. E. Hansen, J. Phys. B **20**, 6541 (1987).

[9]K. Ichikawa, O. Aita, K. Aoki, M. Kamada, and K. Tsutsumi, Phys. Rev. B **45**, 3221 (1992); M. Kamada, K. Ichikawa, and O. Aita, *ibid.* **47**, 3511 (1993).

[10]H. Ogasawara, A. Kotani, B. T. Thole, K. Ichikawa, O. Aita, and M. Kamada, Solid State Commun. **81**, 645 (1992).

[11]J. N. Andersen, O. Björneholm, A. Sandell, R. Nyholm, J. Forsell, L. Thånell, A. Nilsson, and N. Mårtensson, Synch. Radiat. News **4**, 15 (1991).

[12]T. H. DiStefano and W. E. Spicer, Phys. Rev. B **7**, 1554 (1973).

[13]G. W. Rubloff, Phys. Rev. B **5**, 662 (1972).

[14]D. W. Lynch and G. G. Olson, Solid State Commun. **12**, 661 (1973).

[15]A. A. Nikitin and Z. B. Rudzikas, *Foundations of the Theory of the Spectra of Atoms and Ions* (Nauka, Moscow, 1983).

[16]A. C. Parry-Jones, P. Weightman, and P. T. Andrews, J. Phys. C **12**, 1587 (1979).

[17]R. E. Watson, Phys. Rev. **111**, 1108 (1958).

[18]W. van Gool and A. G. Piken, J. Mater. Sci. **4**, 95 (1969).

[19]G. D. Mahan, Phys. Rev. B **21**, 4791 (1980).

[20]N. V. Starostin and V. G. Ganin, Fiz. Tverd. Tela **16**, 572 (1974) [Sov. Phys. Solid State **16**, 369 (1974)].

[21]N. F. Mott and R. W. Gurney, *Electronic Processes in Ionic Crystals* (Clarendon, Oxford, 1948).

[22]Q. C. Johnson and D. H. Templeton, J. Chem. Phys. **34**, 2004 (1961).

[23]J. R. Igel, M. C. Wintergill, J. J. Fontanella, A. V. Chadwik, C. G. Andeen, and V. E. Bean, J. Phys. C **15**, 7215 (1982).

[24]R. D. Deslattes, Phys. Rev. Lett. **20**, 483 (1968).

[25]J. P. Connerade and R. C. Karnatak, J. Phys. F **11**, 1539 (1981); P. Motais, E. Belin, and C. Bonnelle, *ibid.* **11**, L159 (1981).

[26]J. P. Connerade, in *Giant Resonances in Atoms, Molecules, and Solids,* edited by J. P. Connerade, J. M. Esteva, and R. C.

Karnatak (Plenum, New York, 1987), pp. 3–23.
[27]H. Aksela and S. Aksela, Phys. Rev. A **27**, 1503 (1983).
[28]J. Väyrynen and E. Minni, J. Electron Spectrosc. Relat. Phenom. **34**, 275 (1984).
[29]M. Kellokumpu and H. Aksela, Phys. Rev. A **31**, 777 (1985).
[30]E. J. McGuire, Phys. Rev. A **5**, 1043 (1972).
[31]K. Siegbahn, C. Nordling, G. Johanson, J. Hedman, P. F. Heden, K. Hamrin, U. Gelius, T. Bergmark, L. O. Werme, R. Manne, and Y. Baer, *ESCA Applied to Free Molecules* (North-Holland, Amsterdam, 1969).
[32]A. Kotani, T. Jo, and J. C. Parlebas, Adv. Phys. **37**, 37 (1988).
[33]S. Suzuki, T. Ishii, and T. Sagawa, J. Phys. Soc. Jpn. **37**, 1334 (1974).
[34]P. Motais, E. Belin, and C. Bonnelle, Phys. Rev. B **30**, 4399 (1984).
[35]J. C. Riviere, F. P. Netzer, G. Rosina, and G. Strasser, J. Electron Spectrosc. Relat. Phenom. **36**, 331 (1985).
[36]M. Qvarford, J. N. Andersen, R. Nyholm, J. F. van Acker, E. Lundgren, I. Lindau, S. Söderholm, H. Bernhoff, U. O. Karlsson, and S. A. Flodström, Phys. Rev. B **46**, 14 126 (1992).
[37]R. Ruus, A. Kikas, A. Maiste, E. Nõmmiste, A. Saar, M. Elango, J. F. van Acker, M. Qvarford, J. N. Andersen, R. Nyholm, and I. Martinson (unpublished).
[38]U. Gelius, J. Electron Spectrosc. Relat. Phenom. **5**, 985 (1974).
[39]J. Tulkki, T. Åberg, S. B. Whitfield, and B. Crasemann, Phys. Rev. A **41**, 181 (1990); W. Eberhardt, S. Bernstorff, H. W. Jochims, S. B. Whitfield, and B. Crasemann, *ibid.* **38**, 3808 (1988).